Available online at www.sciencedirect.com
SCIENCE DIRECT®
Journal of Sound and Vibration 284 (2005) 299–323
JOURNAL OF SOUND AND VIBRATION
www.elsevier.com/locate/jsvi

A fuzzy approach for the analysis of unbalanced nonlinear rotor systems

Yazhao Qiu, Singiresu S. Rao*

Department of Mechanical Engineering, University of Miami, Coral Gables, FL 33124-0624, USA

Received 23 December 2003; accepted 15 June 2004
Available online 15 December 2004

Abstract

The components of most structural and mechanical systems exhibit considerable variations or uncertainties in their properties. Thus, the performance characteristics of such systems are also subject to uncertainties. In the case of a rotor-bearing system, the nonlinear bearing restoring force is usually represented as a third or fourth power of displacement or as a piecewise linear function of displacement. The coefficients of these models are acquired from experiments and approximations, and will vary considerably during the operation of the bearing. Hence, it is more reasonable to treat them as uncertain values. Other bearing parameters such as the inertial properties of concentrated disks, distributed mass and damping of the rotating assemblies are also uncertain due to manufacturing and assembly errors and imprecise operating conditions. It is known that the vibration response of a rotor is highly sensitive to small fluctuations or variations in the bearing parameters. Therefore, any realistic analysis and design of rotor-bearing systems must take the uncertainties into account. In this paper, a methodology is presented for the fuzzy analysis of nonlinear rotor-bearing systems along with numerical results to demonstrate the computational feasibility of the methodology.
© 2004 Elsevier Ltd. All rights reserved.

1. Introduction

Most components of a rotor-bearing system are subject to variability and uncertainty in real life. For example, the manufacturing of all machine parts involves tolerances and the

*Corresponding author. Tel.: +1 305 254 2571; fax: +1 305 284 2580.
E-mail address: srao@miami.edu (S.S. Rao).

0022-460X/$ - see front matter © 2004 Elsevier Ltd. All rights reserved.
doi:10.1016/j.jsv.2004.06.029

exact dimensions of a machined part can never be predicted. The exact actions such as bearing loads and rotational speeds are subject to variations. The lubricant properties such as density and viscosity fluctuate with the operating conditions such as temperature. The performance characteristics of components such as rollers, balls and shafts vary (degrade) during their lifetimes because of aging, creep, wear, corrosion and changes in operating conditions.

The uncertainty or imprecision present in rotor-bearing systems can be modeled using probabilistic, interval or fuzzy methods. When the uncertain parameters are described as random variables with known probability distributions, the probabilistic methods can be used. If the parameters are denoted by simple ranges, the interval methods can be used for the analysis of the system. If each uncertain parameter is described by a range with preferences specified for different values within the range, the fuzzy approach can be used. The fuzzy analysis can also be used when the parameters are described using linguistic and vague terms such as ''nearly'', ''about'', ''almost'' and ''substantially larger''. This work presents a methodology for the fuzzy analysis of unbalanced nonlinear rotor-bearing systems.

The analysis and design of nonlinear rotor systems have received considerable attention recently. When deflections become large, unexpected phenomena due to nonlinearity may occur and a simple linear model will not be adequate in many applications. Many of the mechanical elements of a rotor system contribute to the nonlinearity of the system in different ways. For example, the clearance in a ball bearing, oil film thickness in a journal bearing, clearance in a squeeze-film damper bearing, and the magnetic force between rotor and the stator may introduce nonlinearity. Additional sources of discontinuous, piecewise nonlinearity may be activated by the motion of the system, based on the operating conditions of the rotor-bearing system. For instance, a loose joint in the system may cause the rotor to rub against the stator occasionally. In such cases, the stiffness of the system varies between two extreme values; with higher stiffness occurring when there is contact at the joint (or rubbing location) and lower stiffness occurring when there is separation between the substructures. The system damping characteristics also alternate in a similar manner. An oversized and poorly lubricated bearing in which the rotor/bearing contact is occasionally interrupted is another example in which the stiffness and damping characteristics vary.

Nonlinear rotor systems generally possess characteristics that are totally different from those of linear systems. In particular, the method of superposition is not valid; thus all excitation sources of interest must be considered simultaneously in a nonlinear system. Multiple solutions may exist for certain areas of parameter space and the nature of stability of each solution may be different. The possibilities always exist for a nonlinear rotor system to exhibit a variety of behaviors such as jump phenomenon, multiple attractors, subharmonic, bifurcation, periodic, quasi-periodic and even chaotic vibrations. All these phenomena can be observed from experiments but cannot be predicted by linear models.

Considerable research has been conducted in the area of nonlinear rotor systems. Yamamoto et al. [1,2] used the harmonic balance method to study the subharmonic and superharmonic vibrations of a two degree of freedom rotor mounted on nonlinear ball bearings. Muszynska and Goldman studied synchronous and subsynchronous periodic as well as chaotic vibrations numerically and experimentally [3]. Lee et al. performed the steady-state analysis of a nonlinear

system using a modified transfer matrix method [4]. Chu et al. investigated the bifurcations and stability of a system with pedestal looseness and rub-impact using Fourier series and Floquet theory. In most cases, a nonlinear model is developed for an element that is expected to exhibit a nonlinear behavior. For example, the restoring force of ball bearings is usually modeled by a third or fourth power [1] of deflection, or as a piecewise discontinuous model [5]. Oil film bearings are assumed to have more complicated nonlinear behavior. All the models have been developed from experiments and approximations. The parameters of these models can vary over wide ranges under different conditions. Thus, a treatment of these coefficients as uncertain parameters will be more realistic and reasonable. In addition, nonlinear systems are basically not deterministic since chaotic motion is always possible in a nonlinear system. The system response may undergo almost instantaneous changes, while one or more system parameters slowly vary in value. For instance, the system that originally responded chaotically to a periodic excitation may unexpectedly self-synchronize into a stable periodic motion, or, in other cases, an initially narrow band of chaos may suddenly increase in bandwidth. This means that nonlinear systems are more sensitive to parameter uncertainties than linear systems. Thus, the use of an uncertainty model appears necessary for the analysis of nonlinear systems. In this work, a fuzzy model is proposed for the vibration analysis of nonlinear rotor-bearing systems.

In rotating machines, nonlinear spring characteristics appear due to various causes as stated earlier. When the restoring force is expressed as a function of the deflection, the nonlinearity is often classified into two types; it is called weak nonlinearity when the deviation from a linear relationship is small, and is called strong nonlinearity when it deviates appreciably from a linear relationship.

Fig. 1 shows two cases of spring characteristics that are obtained when the lower end of an elastic shaft is supported by two different types of bearings. The upper end is supported by a double-row self-aligning ball bearing in both the cases. Fig. 1(a) denotes a case where the lower end is supported by a double-row self-aligning ball bearing. As the inner surface of the outer ring forms part of a sphere, the inner ring can turn freely and the supporting condition will be a simple support. In this case, the spring characteristic of the shaft will be linear. Fig. 1(b) indicates the case where the lower end is supported by a single-row deep-groove ball bearing. Because the balls roll

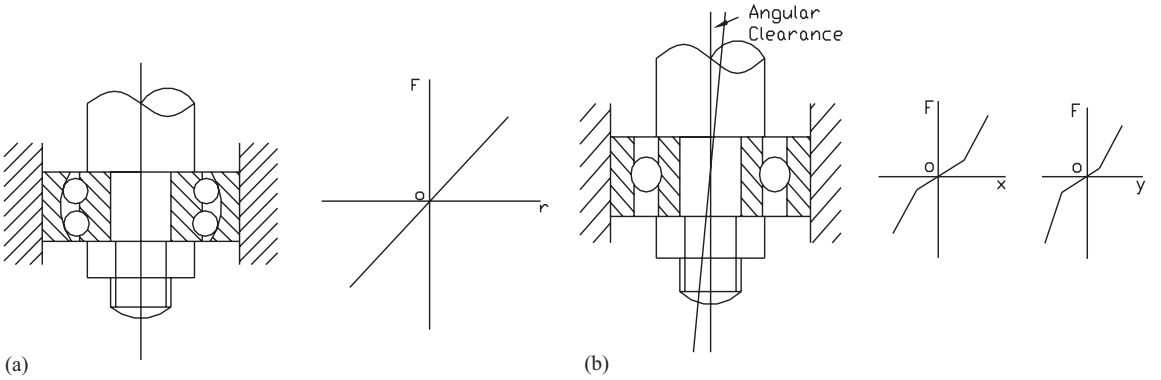

Fig. 1. Ball bearing: (a) with linear spring characteristics, and (b) with weak nonlinearity spring characteristics [2].

in the grooves carved in both the inner and outer rings, the inner ring cannot incline relative to the outer ring and therefore the supporting condition will be a fixed support. However, due to the small clearances present among the inner ring, balls, and the outer ring, the inner ring can incline slightly and the supporting condition becomes a simple support within this clearance. In bearing engineering, the terms radial clearance and axial clearance are commonly used to express the accuracy of bearings. But as it is most convenient to express the clearance by an angle in the treatment of restoring force, the term angular clearance is used in vibration engineering. This angular clearance exists in every direction and can be expressed by a cone as shown in Fig. 1(b). The supporting condition is a simple support when the centerline of the shaft is located in this cone and becomes a fixed support when it is out of the cone. Thus, the restoring force will have the nonlinear characteristics of a piecewise linear type, as shown in Fig. 1(b). In a practical setup, the transition from a simple support to a fixed support occurs gradually because clearances around each ball disappear one by one as the inclination of the shaft increases. Therefore, the practical transition is comparatively smooth and the spring characteristics can be approximated by a power series of low order. Hence, the setup shown in Fig. 1 is generally assumed to have a weak nonlinearity.

Some machine elements cause strong nonlinearity in the system. For example, since ball or roller bearings have little damping effect, aircraft gas turbine engines generally adopt squeeze film damper bearings for some of their bearings. A simplified model of such a bearing is shown in Fig. 2. Damper oil is supplied between the bearing holder A and the casing B. Holder A is supported by a weak spring S and is kept at the center of the casing B. When the shaft vibrates, element A moves relative to element B, and therefore the oil dampens the vibration. When this type of bearing is used in the rotor system, the relationship between the rotor radial deflection r and the restoring force F shows strong nonlinearity with a deadband as indicated [2].

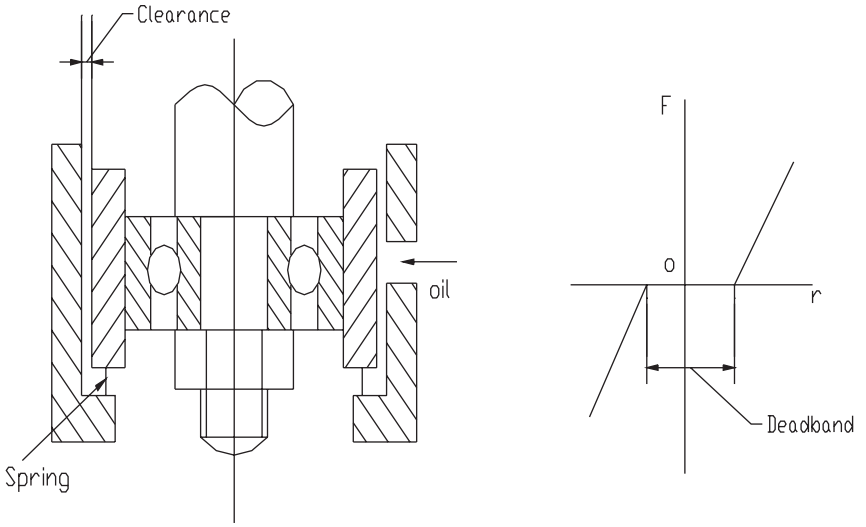

Fig. 2. Ball bearing with strong nonlinearity in spring characteristics [2].

2. Basic concepts of fuzzy mathematics

Fuzzy set theory was initiated by Zadeh [8] and developed by many other researchers, including Kaufmann and Gupta [9]. The basic concepts of fuzzy numbers and fuzzy arithmetic operations are presented below.

2.1. Fuzzy numbers and membership functions

Let $\boldsymbol{X}$ be a classical (crisp) set of objects, called universe, whose generic elements are denoted x. Membership in a classical subset $\boldsymbol{A}$ of $\boldsymbol{X}$ can be viewed as a characteristic function from $\boldsymbol{X}$ to $\{0,1\}$ such that

$$\mu_A(x) = \begin{cases} 1 & \text{if } x \in \boldsymbol{A}, \\ 0 & \text{if } x \notin \boldsymbol{A}. \end{cases} \tag{1}$$

The set $\{0,1\}$ is known as a valuation set. A set $\boldsymbol{A}$ is referred to as a fuzzy set if the valuation set is allowed to be real interval [0,1]. The fuzzy set $\boldsymbol{A}$ is completely characterized by the set of pairs

$$\boldsymbol{A} = \{(x, \mu_A(x)), x \in \boldsymbol{X}\}, \quad 0 \leqslant \mu_A(x) \leqslant 1, \tag{2}$$

where $\mu_A(x)$ is called the grade (or level) of membership function or degree of compatibility of x to $\boldsymbol{A}$. The closer the value of $\mu_A(x)$ is to 1, the more x belong to $\boldsymbol{A}$. Obviously, $\boldsymbol{A}$ is a subset of $\boldsymbol{X}$ that has no sharp boundary. For example, let $\boldsymbol{X}=\{4.00\ 4.02\ 4.04\ 4.06\ 4.08\ 4.10\ 4.12\ 4.14\ 4.16\ 4.18\ 4.20\}$ be possible values of film thickness of the lubricant in a rotor-bearing system (in μm). Then the fuzzy set $\boldsymbol{A}$ of "desirable film thickness to achieve a specific bearing characteristic (Sommerfeld) number" may be defined by a certain tribologist in a specific design as

$$\begin{aligned} \boldsymbol{A} = \{&(4.00, 0.0),\ (4.02, 0.4),\ (4.06, 0.8),\ (4.08, 0.95),\ (4.10, 0.75),\ (4.12, 0.65), \\ &(4.14, 0.5),\ (4.16, 0.4),\ (4.18, 0.2),\ (4.20, 0.0)\}, \end{aligned}$$

where a grade of membership 1 implies complete achievement and 0 implies complete nonachievement of the specific bearing characteristic number.

Fuzzy numbers can be regarded as an extension of crisp (real) numbers. The membership function for a fuzzy number is defined over the interval between 0 and 1 instead of either 0 or 1 for a real number. For numerical applications, a fuzzy number is approximated by sets of closed intervals, known as intervals of confidence, that are denoted by pairs of the lower and upper bounds with respect to specific α-cut subsets. If $\boldsymbol{F}$ if a fuzzy number with a membership function μ_F, then the α-cut is defined as the set

$$\boldsymbol{F}_\alpha = \{x \in \boldsymbol{X}, \mu_F(x) \geqslant \alpha\}. \tag{3}$$

For the ith α-cut, the lower and upper bounds $(\underline{f}, \bar{f})$ are given by

$$\underline{f} = \min\{f : f \in F_\alpha\}, \quad \bar{f} = \max\{f : f \in F_\alpha\}. \tag{4}$$

If a set of α-levels is constructed for all fuzzy quantities in a given problem, each of these quantities may be represented by a 2 by n array as follows (see Fig. 3):

$$\boldsymbol{F} = \{(\underline{f}, \bar{f})_{\alpha_1},\ (\underline{f}, \bar{f})_{\alpha_2}, \ldots, (\underline{f}, \bar{f})_{\alpha_n}\}. \tag{5}$$

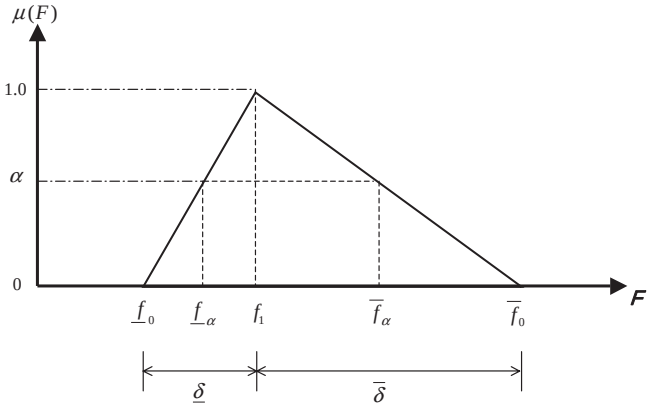

Fig. 3. Triangular fuzzy number.

In addition, each fuzzy number possesses two attributes: convexity and normality. Convexity requires that the shape of a membership function be convex. Normality implies the highest grade of membership function to be equal to 1.

2.2. Fuzzy arithmetic operations

Fuzzy arithmetic is based on the extension principle. The computational features of the extension principle can be achieved by using the α-cut representation of fuzzy numbers. Since any fuzzy number can be represented in interval form, as indicated in Eq. (5), fuzzy arithmetic operations can be implemented using interval (operation) analysis at each of the n α-levels independently. The solution of fuzzy arithmetic equations will be the result of interval operations carried out by a nested family of intervals for each fuzzy number. All the rules used for interval arithmetic are equally applicable to fuzzy arithmetic at each α-level.

If **A** and **B** are two fuzzy numbers, their union is defined as the set whose members have the maximum of the two membership values: $\mu_{A\cup B} = \mu_A \vee \mu_B$ and the intersection operation chooses the minimum of the two membership values: $\mu_{A\cap B} = \mu_A \cdot \mu_B$, where $X \cdot Y$ means minimum of X and Y and $X \vee Y$ means maximum of X and Y. Fuzzy arithmetic operations include fuzzy addition, fuzzy subtraction, fuzzy multiplication, and fuzzy division. In this work, fuzzy arithmetic operations are denoted as (**), where ** represents deterministic arithmetic operations such as $+$, $-$, *,/. Thus, $+$ denotes the deterministic addition while $(+)$ represents the fuzzy addition. A bold face letter is used to denote fuzzy number; for example, x indicates a deterministic number while **x** denotes a fuzzy number. Fuzzy arithmetic operations have features that are different from those of deterministic arithmetic. Fuzzy addition and fuzzy multiplication are commutative, associative and distributive, but neither fuzzy subtraction nor fuzzy division is associative because $\mathbf{A}(-)\mathbf{B}(+)\mathbf{B} \neq \mathbf{A}$, and $[\mathbf{A}(/)\mathbf{B}](\cdot)\mathbf{B} \neq \mathbf{A}$. Also, a fuzzy zero **0** is defined as a fuzzy number in which the value zero has a membership value of one, the left and right numbers of zero may not be the same. Similarly, a fuzzy one **1** is defined as a fuzzy number in which the value one has a membership value of one, the left and right numbers of one may not be the same. The fuzzy

arithmetic operation of two fuzzy numbers A and B is

$$\mathbf{A}(^{**})\mathbf{B} = \mu_{\mathbf{A}(^{**})\mathbf{B}}(z) = \bigvee_{z=x^{**}y} (\mu_{\mathbf{A}}(x) \wedge \mu_{\mathbf{B}}(y)), \tag{6}$$

which can also be expressed as

$$\begin{aligned}
&\mathbf{A}_\alpha(+)\mathbf{B}_\alpha = [a_\alpha^- + b_\alpha^-, a_\alpha^+ + b_\alpha^+] \quad \text{for } \mathbf{A}_\alpha, \mathbf{B}_\alpha \in IR,\\
&\mathbf{A}_\alpha(-)\mathbf{B}_\alpha = [a_\alpha^- - b_\alpha^+, a_\alpha^+ - b_\alpha^-] \quad \text{for } \mathbf{A}_\alpha, \mathbf{B}_\alpha \in IR,\\
&\mathbf{A}_\alpha(\cdot)\mathbf{B}_\alpha = \begin{cases}
\left[a_\alpha^{-\sigma(\mathbf{B}_\alpha)} b_\alpha^{-\sigma(\mathbf{A}_\alpha)}, a_\alpha^{\sigma(\mathbf{B}_\alpha)} b_\alpha^{\sigma(\mathbf{A}_\alpha)}\right] & \text{for } \mathbf{A}_\alpha, \mathbf{B}_\alpha \in IR\backslash Z,\\
\left[a_\alpha^{\delta} b_\alpha^{-\delta}, a_\alpha^{\delta} b_\alpha^{\delta}\right], \delta = \sigma(\mathbf{A}_\alpha) & \text{for } \mathbf{A}_\alpha \in IR\backslash Z, \mathbf{B}_\alpha \in Z,\\
\left[a_\alpha^{-\delta} b_\alpha^{\delta}, a_\alpha^{\delta} b_\alpha^{\delta}\right], \delta = \sigma(\mathbf{B}_\alpha) & \text{for } \mathbf{A}_\alpha \in Z, \mathbf{B}_\alpha \in IR\backslash Z,\\
\left[\min\{a_\alpha^- b_\alpha^+, a_\alpha^+ b_\alpha^-\}, \max\{a_\alpha^- b_\alpha^-, a_\alpha^+ b_\alpha^+\}\right] & \text{for } \mathbf{A}_\alpha, \mathbf{B}_\alpha \in Z,
\end{cases}\\
&\mathbf{A}_\alpha(/)\mathbf{B}_\alpha = \begin{cases}
\left[a_\alpha^{-\sigma(\mathbf{B}_\alpha)} / b_\alpha^{\sigma(\mathbf{A}_\alpha)}, a_\alpha^{\sigma(\mathbf{B}_\alpha)} / b_\alpha^{-\sigma(\mathbf{A}_\alpha)}\right] & \text{for } \mathbf{A}_\alpha, \mathbf{B}_\alpha \in IR\backslash Z\\
\left[a_\alpha^{-\delta} / b_\alpha^{-\delta}, a_\alpha^{\delta} / b_\alpha^{-\delta}\right], \delta = \sigma(\mathbf{B}_\alpha) & \text{for } \mathbf{A}_\alpha \in Z, \mathbf{B}_\alpha \in IR\backslash Z,
\end{cases}
\end{aligned} \tag{7}$$

where $\mathbf{A}_\alpha$ and $\mathbf{B}_\alpha$ are the intervals of confidence of $\mathbf{A}$ and $\mathbf{B}$, respectively, for the level of presumption $\alpha,\alpha\in[0,1]$, $\mathbf{A}_\alpha = \{x|\mu_{\mathbf{A}}(x)\geqslant\alpha\} = [a_\alpha^-, a_\alpha^+]$ and $\mathbf{B}_\alpha = \{x|\mu_{\mathbf{B}}(x)\geqslant\alpha\} = [b_\alpha^-, b_\alpha^+]$. IR is the set $\{[a,b]|a,b\in R, a\leqslant b\}$ of all intervals. The superscripts $^-$ and $^+$ denote the lower and upper bounds of the interval, respectively. Z denotes the set of intervals that contain zero as $Z = \{A \in IR|0 \in A\} = \{A|a^- \leqslant 0 \text{ and } a^+ \geqslant 0\}$ while the set of intervals which do not contain zero is denoted as $IR\backslash Z$. σ is a sign function defined as $\sigma(A) = \{+, \text{ if } a^- > 0;\ -, \text{ if } a^+ < 0\}$.

The powers of a fuzzy number are computed by repetitive multiplication operations. Summation of fuzzy numbers is computed by repetitive additions. Fuzzy root (fuzzy inverse, fuzzy absolute value), is evaluated by taking the root (reciprocal value, absolute value) of each element of the fuzzy number, without changing the associated membership values. For trigonometry operations, for $\mathbf{X}_\alpha = [x_1^\alpha,\ x_2^\alpha]$, the following equations are defined:

$$\begin{aligned}
&\cos(\mathbf{X}_\alpha) = [\cos(x_2^\alpha), \quad \cos(x_1^\alpha)], \quad x_1^\alpha, x_2^\alpha \in [0,\ \pi/2],\\
&\sin(\mathbf{X}_\alpha) = [\sin(x_1^\alpha), \quad \sin(x_2^\alpha)], \quad x_1^\alpha, x_2^\alpha \in [0,\ \pi/2],\\
&\cosh(\mathbf{X}_\alpha) = [\cosh(x_1^\alpha), \quad \cosh(x_2^\alpha)], \quad x_1^\alpha, x_2^\alpha \in R^+,\\
&\sinh(\mathbf{X}_\alpha) = [\sinh(x_1^\alpha), \quad \sinh(x_2^\alpha)], \quad x_1^\alpha, x_2^\alpha \in R.
\end{aligned} \tag{8}$$

3. Equations of motion

Consider a Jeffcott rotor model using nonlinear ball bearings as shown in Fig. 4 [6] with a rigid disk of mass M and flexible shaft segments of identical length L on each side of the disk. The shaft segments are assumed to have negligible mass with a bending stiffness EI. The equations of

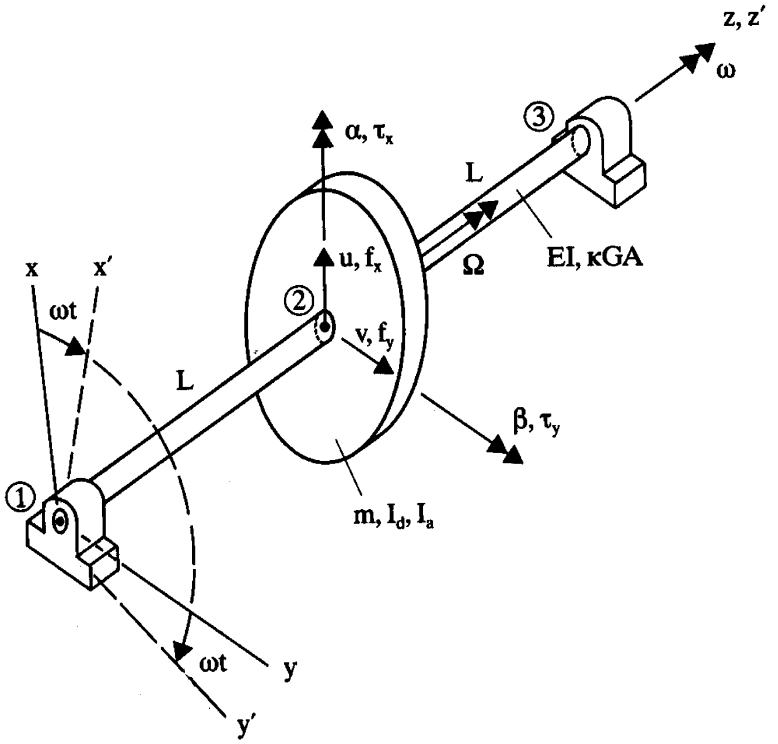

Fig. 4. Jeffcott rotor model [6].

motion can be written as

$$M\ddot{u} + k_T u = f_u, \quad M\ddot{v} + k_T v = f_v, \tag{9}$$

where u and v denote the components of displacement parallel to x and y axes, respectively, k_T indicates the translational stiffness coefficient

$$k_T = \frac{6EI}{(1+3\varepsilon)L^3} \tag{10}$$

and the factor $\varepsilon = EI/(\kappa GAL^2)$ is a dimensionless measure of the shear compliance of the segment. When shear compliance is neglected, as in Bernoulli–Euler beam theory, $G \to \infty$ and $\varepsilon \to 0$. Usually, the excitation of a rotor system is caused by an out of balance mass, so the forces on the right-hand side of Eq. (9) can be defined as

$$f_u = f_{eu} + f_{bu}, \quad f_v = f_{ev} + f_{bv}, \tag{11}$$

where the subscripts e and b denote the mass unbalance and bearing forces, respectively. The mass unbalance forces are given by

$$f_{eu} = me\Omega^2 \cos(\Omega t + \varphi_0), \; f_{ev} = me\Omega^2 \sin(\Omega t + \varphi_0), \tag{12}$$

when the mass m is situated at a distance e from the geometric center of the shaft. The restoring forces in the x and y directions can be expressed, in a general form, as [2]

$$f_u = c_1u^2 + c_2uv + c_3v^2 + c_4u^3 + c_5u^2v + c_6uv^2 + c_7v^3,$$
$$f_v = d_1u^2 + d_2uv + d_3v^2 + d_4u^3 + d_5u^2v + d_6uv^2 + d_7v^3, \tag{13}$$

where c_i and d_i, $i=1,2,\ldots,7$, are constants. In this work, bearings with weak nonlinearity spring characteristics, as shown in Fig. 1, are considered. In this case the bearing restoring forces are usually modeled by the third power of the displacement, so that the bearing forces can be expressed, including linear damping characteristics, as [10,11]

$$f_{bu} = K_1u + K_3u^3 + C\dot{u}, \quad f_{bv} = K_1v + K_3v^3 + C\dot{v}, \tag{14}$$

where K_1 and K_3 are the linear and nonlinear stiffness coefficients and C is the linear damping coefficient. These and other coefficients of the rotor are shown in Fig. 5 and the numerical values of the bearing parameters used in the simulations are listed in Tables 1 and 2.

Assuming

$$S = \begin{Bmatrix} s_1 \\ s_2 \\ s_3 \\ s_4 \end{Bmatrix} \equiv \begin{Bmatrix} u \\ v \\ \dot{u} \\ \dot{v} \end{Bmatrix} \tag{15}$$

and combine Eqs. (9)–(13), the equations of motion can be rewritten as

$$\dot{S} = \begin{Bmatrix} \dot{s}_1 \\ \dot{s}_2 \\ \dot{s}_3 \\ \dot{s}_4 \end{Bmatrix} = \begin{Bmatrix} s_3 \\ s_4 \\ \frac{1}{M}\left\{me\Omega^2\cos(\Omega t+\varphi_0) + K_1s_1 - \frac{6EI}{L^3}s_1 + K_3s_1^3 + Cs_3\right\} \\ \frac{1}{M}\left\{me\Omega^2\sin(\Omega t+\varphi_0) + K_1s_2 - \frac{6EI}{L^3}s_2 + K_3s_2^3 + Cs_4\right\} \end{Bmatrix}. \tag{16}$$

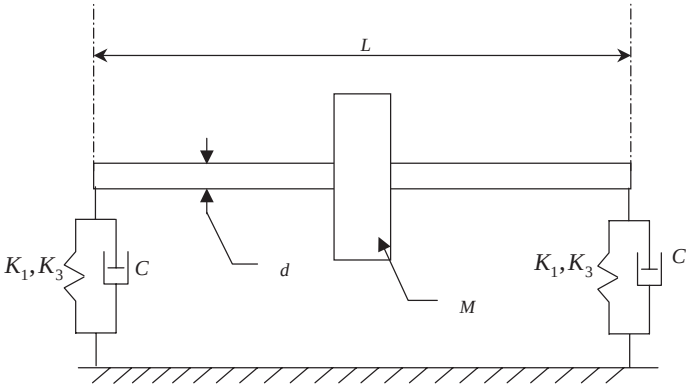

Fig. 5. Computational model of the rotor system.

Table 1
Physical parameters of the system, Example 1

E	$2.0 \times 10^{11}\,\mathrm{N/m^2}$	M	14.29 kg
ρ	$7800\,\mathrm{kg/m^3}$	me	$1.5 \times 10^{-5}\,\mathrm{kg\,m}$
L	0.4 m	K_1	$1.5 \times 10^{6}\,\mathrm{N/m}$
d	0.02 m	C	50 N s/m

Table 2
Physical parameters of the system, Example 2

E	$2.07 \times 10^{7}\,\mathrm{N/cm^2}$	M	10 kg
ρ	$7.75 \times 10^{-3}\,\mathrm{kg/cm^3}$	me	0.04 kg cm
L	30 cm	K_1	$1.5 \times 10^{4}\,\mathrm{N/cm}$
d	0.6 cm	C	60 N s/cm

The fourth-order Runge–Kutta method is used for the solution of Eq. (16). Two numerical examples are considered in this study. The data are shown in Tables 1 and 2. The computations are performed twice; first by assuming the parameters to be crisp (or deterministic) and next by assuming the parameters to be fuzzy (or imprecise). The jump phenomenon is studied in Example 1 and superharmonic and subharmonic responses are studied in Example 2. The frequency response curves corresponding to different nonlinearities near the synchronous resonance are shown in Fig. 6, in which the maximum amplitude of the shaft in one revolution, while rotating at a constant speed, is taken as the response. In order to achieve the steady-state response, a time span equivalent to 100 periods is used and the first 30 periods are treated as the transient response and not used in the computations.

4. Crisp analysis

It can be seen from Fig. 6 that with a hardening spring ($K_3 > 0$) the response curve tends to bend to the right, while with a softening spring ($K_3 < 0$) the curve bends to the left. The damping in the system induces multivalued amplitudes, that is, a jump phenomenon in the frequency response curves. Consider, for example, curve B, which corresponds to a value of $K_3 = 1.5 \times 10^{13}$. The response computations begin at point 1. The steady-state responses of the system are calculated as the speed changes from a lower to a higher value in steps. The response is found to increase monotonically along curve B up to point 2, and then jump to a lower value to point 3 and gradually decrease to point 4. Conversely, when calculations are performed from a higher to a lower speed, that is, from point 4, curves 4–5–6 is realized. The jump phenomenon takes place from points 2 to 3 in the former case and from 5 to 6 in the later case. A similar phenomenon occurs when $K_3 < 0$. During calculations, the steady-state displacement at the current speed (or current iterative step) is taken as the initial condition for the next speed (or step). This procedure is actually a simulation of the real world's operation of increasing the rotational speed slowly,

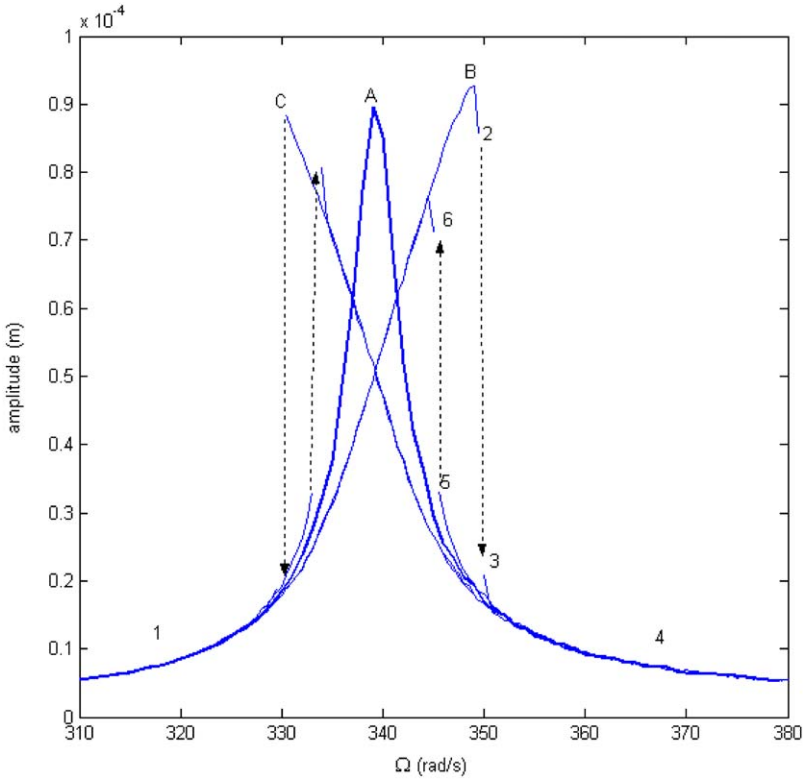

Fig. 6. Frequency response curves corresponding to different nonlinearities (curves A, B and C correspond to $K_3 = 0$, 1.5e13 and -1.5e13, respectively).

passing through the critical speed, and then decreasing the speed slowly. The jump phenomenon was also observed in experiments by many researchers.

Because of the cubic nonlinearity, nonsynchronous $3\times$ whirl or 1/3 whirl are combined with the synchronous whirl in the steady-state response. The superharmonic resonance will occur at rotational speed of $\omega = 1/3\Omega$ and the subharmonic will occur at a speed of $\omega = 3 \times \Omega$ with Ω indicating the critical speed of the corresponding linear system. The orbits of the superharmonic and subharmonic whirls are studied in Example 2. The synchronous critical speed Ω is found to be 39.3 rad/s for the linear system.

The steady-state orbits corresponding to different values of the nonlinear stiffness coefficient are shown in Fig. 7 which contain synchronous ($1\times$) and superharmonic (1/3) whirls at one-third of the critical speed of the corresponding linear system. It can be seen that the orbits become smaller and change into rectangular and even polygonal shape as the value of the nonlinear coefficient increases.

The orbits of responses, which contain synchronous and subharmonic ($3\times$) whirls at three times the critical speed are shown in Fig. 8. It can be seen that as the value of the nonlinear stiffness coefficient becomes smaller, the shape of the whirl approaches a circle as in the case of linear response. With increasing nonlinearity, the orbit changes into complicated forms.

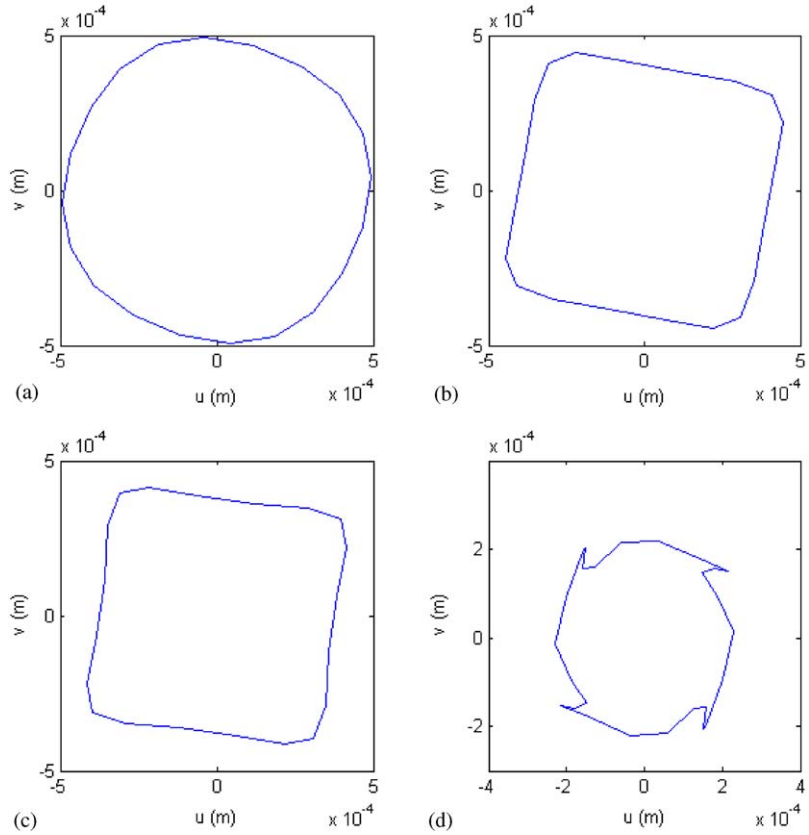

Fig. 7. Whirling orbits at rotational speed, $\Omega = 13.1$ rad/s, for different nonlinearities: (a) with $K_3 = 1.0e9$, (b) $K_3 = 9.0e9$, (c) $K_3 = 1.5e10$, and (d) $K_3 = 5.0e11$.

5. Fuzzy analysis

A framework of fuzzy modeling of mechanical systems is given in reference [12]. In the present work, the response of the rotor-bearing system is studied by considering the parameters to be fuzzy in the two examples. The parameters $\mathbf{k_T}$, $\mathbf{M}$, $\mathbf{me}$, $\mathbf{K_1}$, $\mathbf{K_3}$ and $\mathbf{C}$ are assumed to be fuzzy with triangular membership functions as indicated in Fig. 9. Eq. (16) can be rewritten as

$$\dot{\mathrm{S}} = \begin{Bmatrix} \dot{\mathbf{s}}_1 \\ \dot{\mathbf{s}}_2 \\ \dot{\mathbf{s}}_3 \\ \dot{\mathbf{s}}_4 \end{Bmatrix} = \begin{Bmatrix} \mathbf{s_3} \\ \mathbf{s_4} \\ 1(/)\mathbf{M}(\cdot)\{me\Omega^2 \cos(\Omega t + \varphi_0)(+)\mathbf{K_T}(\cdot)\mathbf{s_1}(+)\mathbf{K_3}(\cdot)\mathbf{s_1}(\cdot)\mathbf{s_1}(\cdot)\mathbf{s_1}(+)\mathbf{C}(\cdot)\mathbf{s_3}\} \\ 1(/)\mathbf{M}(\cdot)\{me\Omega^2 \cos(\Omega t + \varphi_0)(+)\mathbf{K_T}(\cdot)\mathbf{s_2}(+)\mathbf{K_3}(\cdot)\mathbf{s_2}(\cdot)\mathbf{s_2}(\cdot)\mathbf{s_2}(+)\mathbf{C}(\cdot)\mathbf{s_4}\} \end{Bmatrix}. \quad (17)$$

The influence of the individual fuzzy parameters on the response of the system is studied separately. The frequency response curves corresponding to different α-cuts ($\alpha = 0$, 0.25 and 0.75) of two representative parameters are given in Figs. 10 and 11. The maximum variation or interval

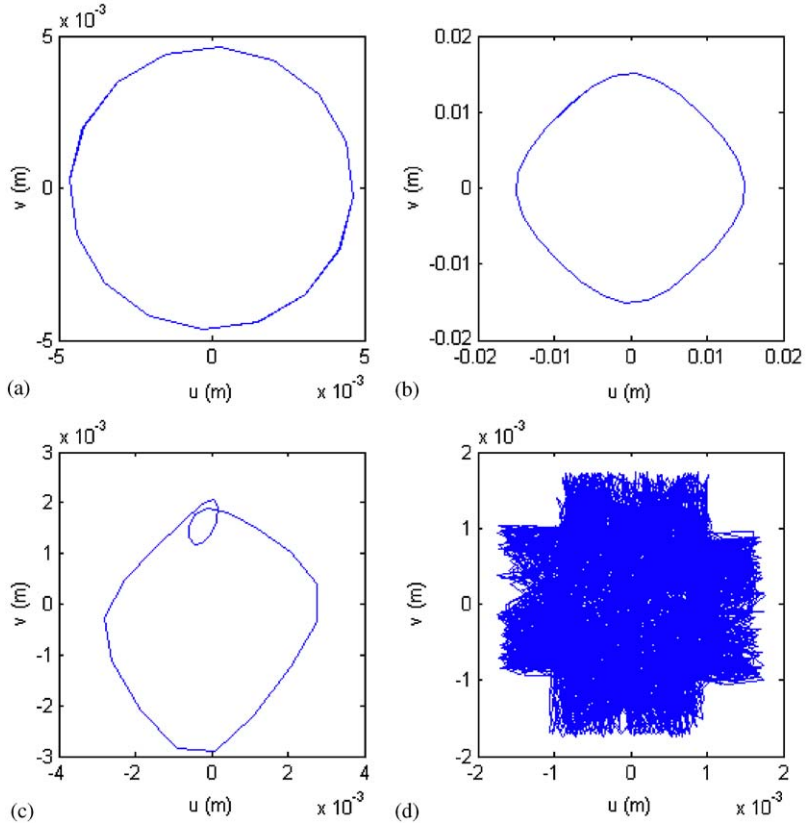

Fig. 8. Whirling orbits at rotational speed $\Omega = 117.9$ rad/s, for different nonlinearities: (a) with $K_3 = 1.0e7$, (b) $K_3 = 1.0e9$, (c) $K_3 = 1.0e11$, and (d) $K_3 = 5.0e11$.

assumed for each parameter, at $\alpha = 0$, is given in Table 3. The variations are assumed to be different for different parameters to reflect the variations encountered in the real world. For example, the uncertainty in mass and mass unbalance is generally caused by the manufacturing and assembly errors, and the ranges of this kind of uncertainties cannot be very large. On the other hand, the stiffness and damping of the system are substantially affected by the clearance, lubricant condition and operating temperature. For light turbine oil, SAE5, for example, a change in temperature from 50 to 60 °C causes the oil viscosity and the Sommerfeld number to vary by 60%. This will result in a change in the bearing stiffness, for a full circular bearing, by 50% [7] A variation of $\pm 10\%$ interval is assumed for K_1 in this study.

Fig. 10 indicates the influence of the uncertainty in k_T. The uncertainty in k_T is caused by the uncertainties of the geometric dimensions of the system and the material properties; specifically, Young's modulus E, diameter of the shaft d and the length of the shaft L (see Eq. (12)). On the other hand, the uncertainty in K_1 is substantially affected by the clearance, lubricant condition and operating temperature, so it can vary by a large amount. Although the uncertainty in K_1 is more important for a flexible shaft, the variations in the two parameters k_T and K_1 are basically

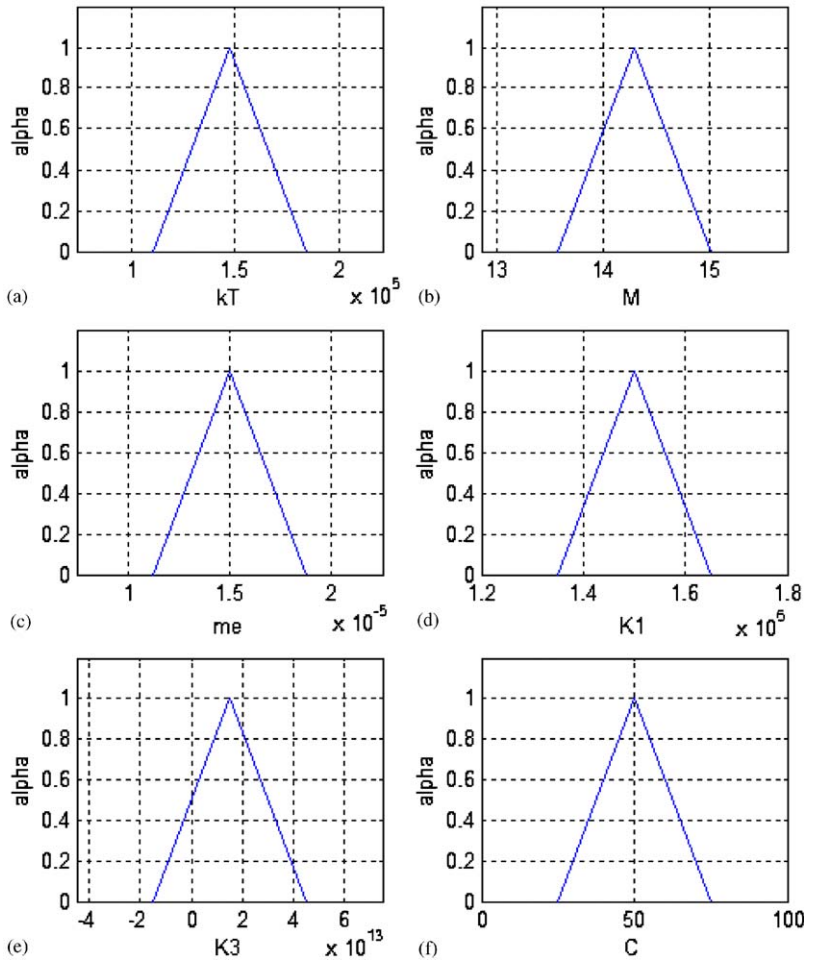

Fig. 9. Membership functions of the fuzzy parameters in Example 1: (a) K_T, (b) M, (c) me, (d) K_1, (e) K_3, (f) C.

found to cause the frequency response curves move horizontally as indicated in Fig. 10 for k_T. When the stiffness of the system is increased, the curve moves to the right and, when it is decreased, the curve moves to the left. This implies that the major influence of the parameters k_T and K_1 is to change the critical speed of the system. The shape of the response curve will not change although the maximum amplitude will increase a little when the stiffness is increased. The membership function of the critical speed, found with k_T considered as fuzzy is shown in Fig. 12.

The influence of uncertainty in the mass of disk M is found to be exactly the opposite of that of stiffness. A comparison of the responses shown in Figs. 11 and 10 indicates that the variation of M will move the response curve horizontally in a direction opposite to the one observed with a variation in the stiffness, that is, when M is increased, the curve will move to the left, and when it is decreased, the curve will move to the right. The membership function of the critical speed, found with M as the only fuzzy input parameter, is shown in Fig. 13. In Fig. 11, the dashed line

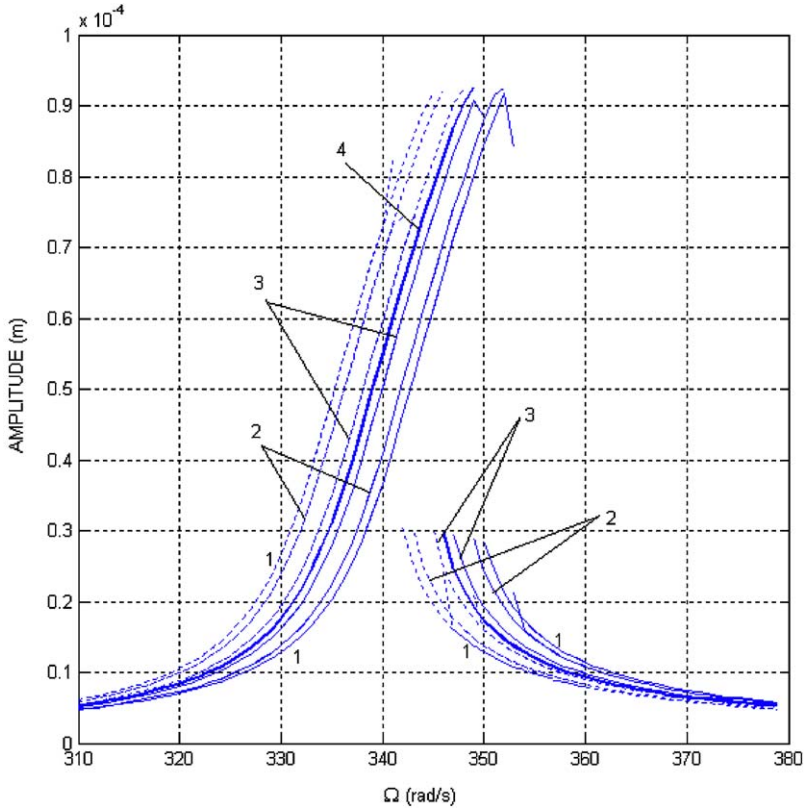

Fig. 10. Response with k_T considered as fuzzy ($\pm 25\%$ variation at $\alpha = 0$): curves 1, 2, 3 and 4 correspond to $\alpha = 0, 0.25, 0.75$ and 1, respectively; dotted lines denote lower bounds and solid lines denote upper bounds.

denotes the opposite effect, which means that the lower bound of the output parameter corresponds to the upper bound of the input parameter.

It is obvious that both mass and linear stiffness will not change the shape of the response curve, implying that they only affect the linear part of the system. Since the uncertainties in these parameters can change the critical speed substantially, they should be considered carefully during the design process of establishing the critical speed of the system.

The uncertainty in the mass unbalance is found to move the response curve vertically by a small amount. The assumed $\pm 25\%$ variation (at $\alpha = 0$) will cause a small interval in the vertical direction, but the maximum amplitude at the critical speed is found to change greatly. The maximum variation in the maximum amplitude is found to be nearly $\pm 27\%$. At the same time, the difference between the two jump speeds (i.e., jump speeds observed with increasing and decreasing rotational speed of the rotor) is also affected. The difference in jump speeds increases with an increase in the uncertainty of the mass unbalance.

Although not shown, the uncertainty in the nonlinear stiffness characteristic is observed to change the response curve greatly. A negative variation in the nonlinear stiffness will bend the

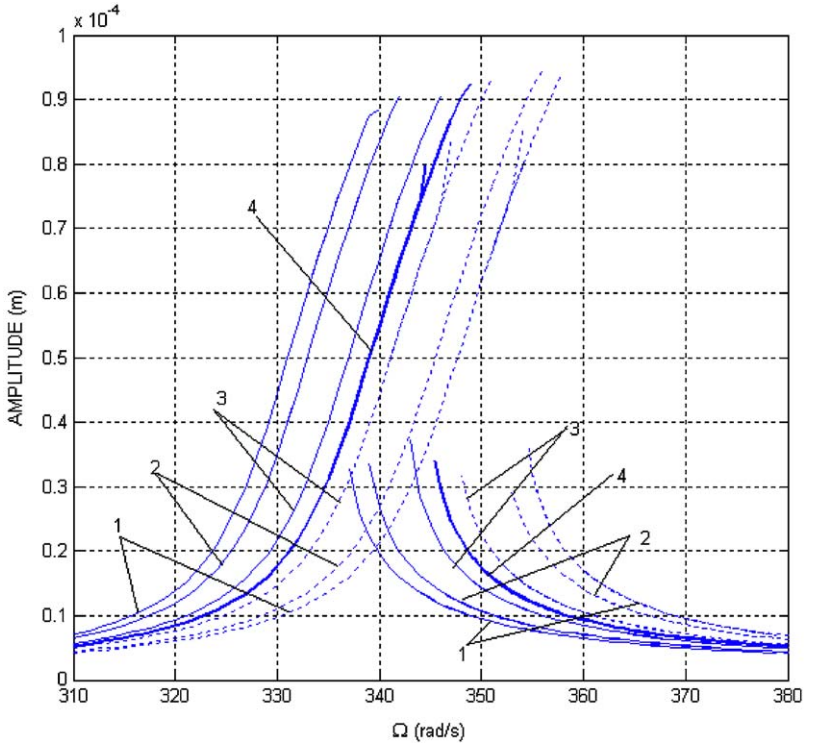

Fig. 11. Response with M considered as fuzzy ($\pm 5\%$ variation at $\alpha = 0$): curves 1, 2, 3 and 4 correspond to $\alpha = 0, 0.25, 0.75$ and 1, respectively; dotted lines denote lower bounds and solid lines denote upper bounds.

Table 3
Maximum variations of fuzzy parameters in Example 1

k_T	M	me	K_1	K_3	C
$\pm 25\%$	$\pm 5\%$	$\pm 25\%$	$\pm 10\%$	$\pm 200\%$	$\pm 50\%$

curve to the left side while a positive variation in the stiffness will cause the curve to bend to the right. The larger the absolute value of K_3, the more the curve will bend. K_3 affects almost all aspects of the response curve, including the shape, critical speed, maximum amplitude and the difference between jump speeds. The membership functions of the critical speed and jump speed difference outputs, found with K_3 as the only fuzzy parameter, are shown in Fig. 14.

The uncertainty in damping is observed to mainly change the critical speed, maximum amplitude and the difference between jump speeds. The membership functions of the maximum amplitude and jump speed difference, found with C as the fuzzy parameter, are shown in Fig. 15.

The intervals of the fuzzy parameters used in Example 2 are given in Table 4. As in the case of Example 1, triangular membership functions are used for the fuzzy input parameters of Example 2.

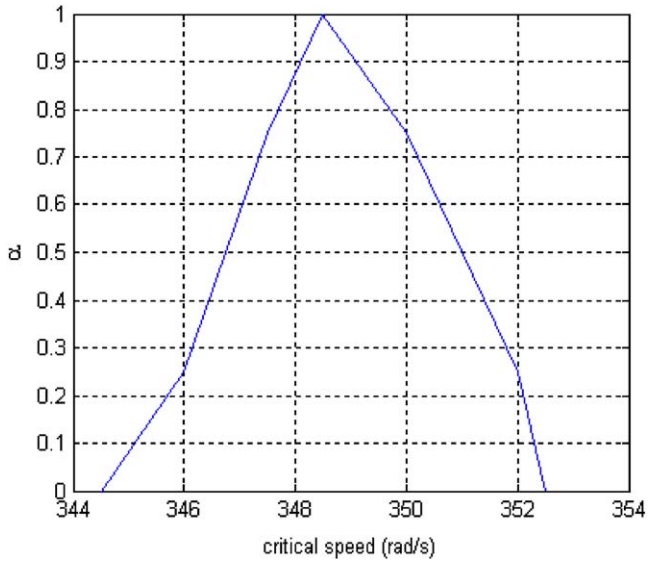

Fig. 12. Membership function of critical speed when k_T is fuzzy.

The influence of the fuzzy input parameters on the subharmonic and superharmonic motion of the system is studied. The whirling orbits are shown in Figs. 16–18 for representative parameters. It has been observed that the superharmonic motion is mainly affected by K_1, K_3, mass unbalance *me* and the damping constant C. The larger the K_1 is, the closer the superharmonic orbit to a circle, which is the orbit of a linear system. When *me* is decreased, the size of the orbit is found to decrease and approach the shape of a circle. As in the deterministic case, an increase in the value of K_3 is found to cause the orbit deviate away from the shape of a circle and approach the shape of a rectangle. At the same time, increasing values of K_3 are found to reduce the size of the orbit. A change in the damping constant seems to just rotate the superharmonic orbit. The subharmonic motion is influenced by the mass unbalance and the value of K_3 in terms of the size of the orbit. Increasing values of *me* are observed to increase the size of the orbit, while increasing values of K_3 are found to decrease the size of the orbit.

Even with weak nonlinearity, the system may exhibit the phenomenon of chaos, when the nonlinear characteristic is large. Fig. 19 gives the bifurcation plot of the vertical displacement of the disk when K_3 is increased to a value of 5.0e11, the system appears to be chaotic. In order to investigate the influence of fuzzy input on the chaos pattern, the damping constant C is treated as the fuzzy input parameter with $\pm 50\%$ variation at $\alpha = 0$. Figs. 20 and 21 give the bifurcation plots corresponding to the lower and upper bound values of C, respectively. The differences can be seen by comparing the results of Figs. 20 and 21 with those shown in Fig. 19. Basically, a lower damping value will cause a broader chaotic area, while a higher damping value will reduce the width of chaotic band. Orbits and Poincaré maps are shown, at $\Omega = 45$ and 111 rad/s for illustration, in Figs. 22 and 23. From Fig. 22, the central and the upper bound values of C can be seen to make the system a period 1 vibration. When C is at its lower bound, the system experiences

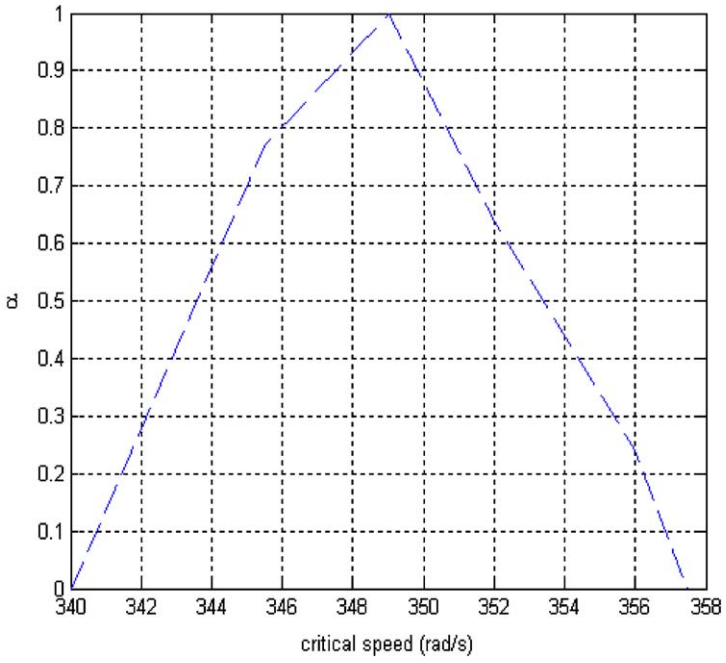

Fig. 13. Membership function of critical speed when M is fuzzy.

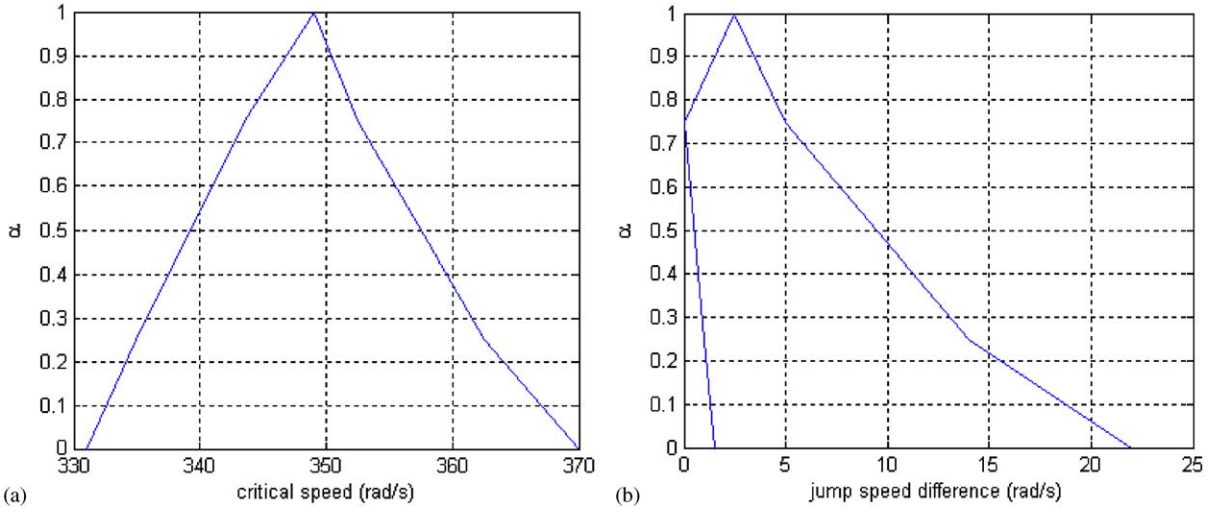

Fig. 14. Membership functions when K_3 is fuzzy: (a) for critical speed, and (b) for jump speed difference.

a period 3 motion. Fig. 23 shows the same trend; when the value of C is decreased to its lower bound value, the system changes from period 3 motion to a chaotic motion.

It is to be noted that the fuzzy analysis of the rotor-bearing system described above has been conducted by assuming linear membership function for the fuzzy parameters. If more information

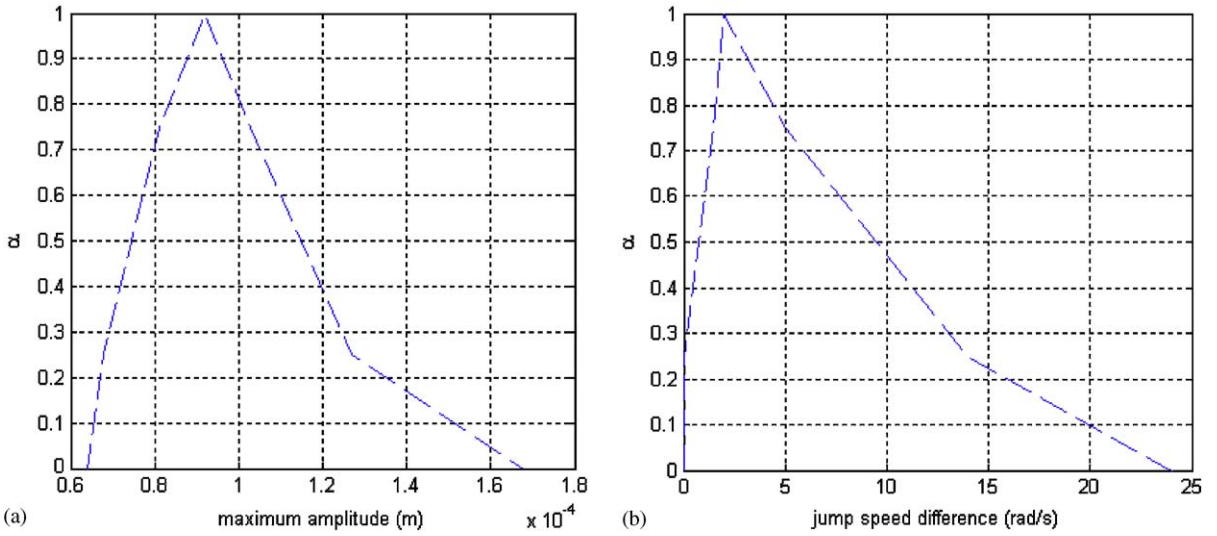

Fig. 15. Membership functions when C is fuzzy: (a) for maximum amplitude, and (b) for jump speed difference.

Table 4
Maximum variations of the fuzzy parameters (at $\alpha = 0$) used in Example 2

k_T	M	me	K_1	K_3	C
$\pm 25\%$	$\pm 5\%$	$\pm 25\%$	$\pm 50\%$	$\pm 50\%$	$\pm 50\%$

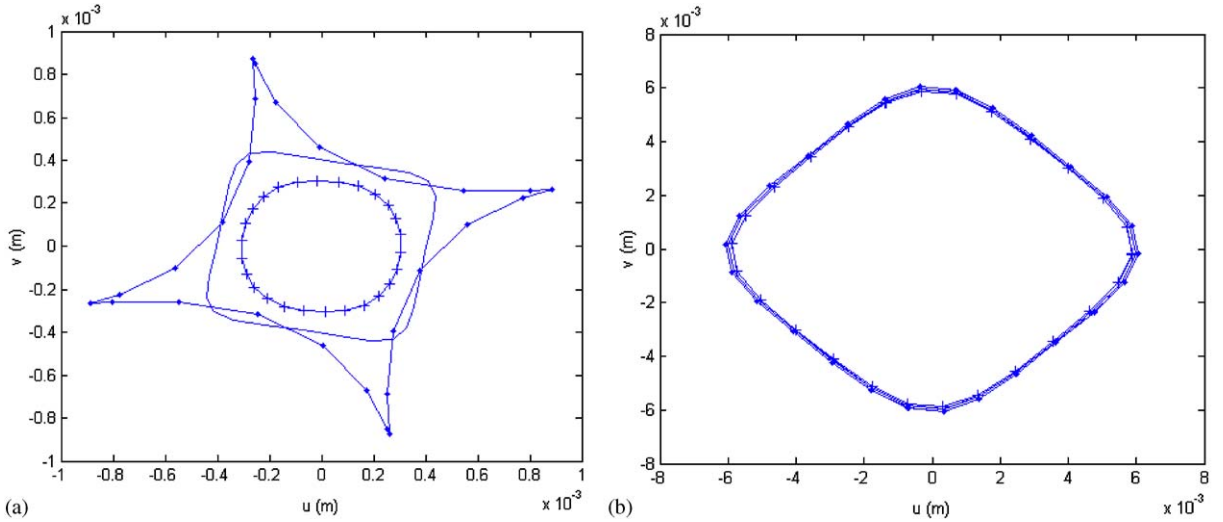

Fig. 16. Orbits with K_1 as fuzzy: (a) when $\Omega = 13.1$ rad/s, and (b) when $\Omega = 117.9$ rad/s (—, center value; –•–, lower bound; –+–, upper bound).

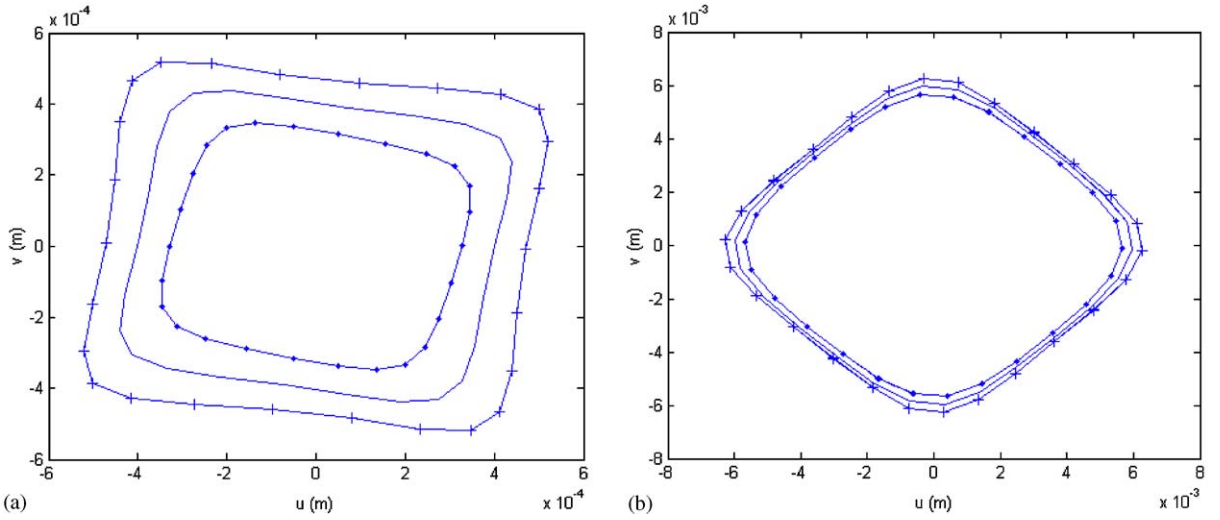

Fig. 17. Orbits with *me* as fuzzy: (a) when $\Omega = 13.1$ rad/s, and (b) when $\Omega = 117.9$ rad/s (—, center value; –•–, lower bound; –+–, upper bound).

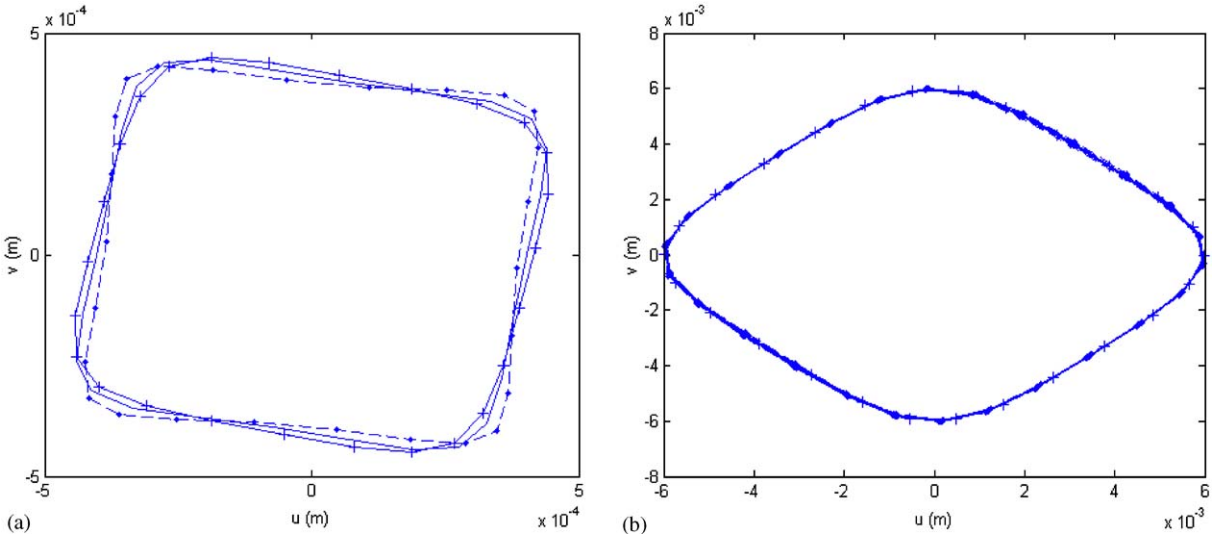

Fig. 18. Orbits with *C* as fuzzy: (a) when $\Omega = 13.1$ rad/s, and (b) when $\Omega = 117.9$ rad/s s (—, center value; –•–, lower bound; –+–, upper bound).

is available on the fuzzy parameters, nonlinear membership functions can be constructed which can then be used in finding the fuzzy response of the system. In some cases, the parameters are described by linguistic statement such as, "the mass unbalance if very low", and "damping in the system is low but not very low". The fuzzy set theory can be conveniently used to manipulate

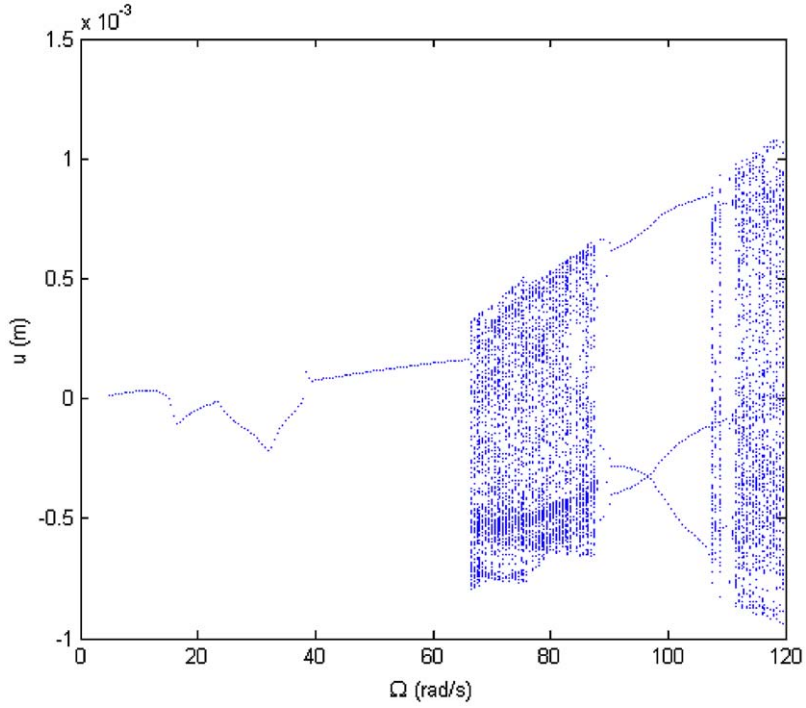

Fig. 19. Bifurcation plot of vertical displacement with $K_3 = 5.0e11$ and $C = 60$.

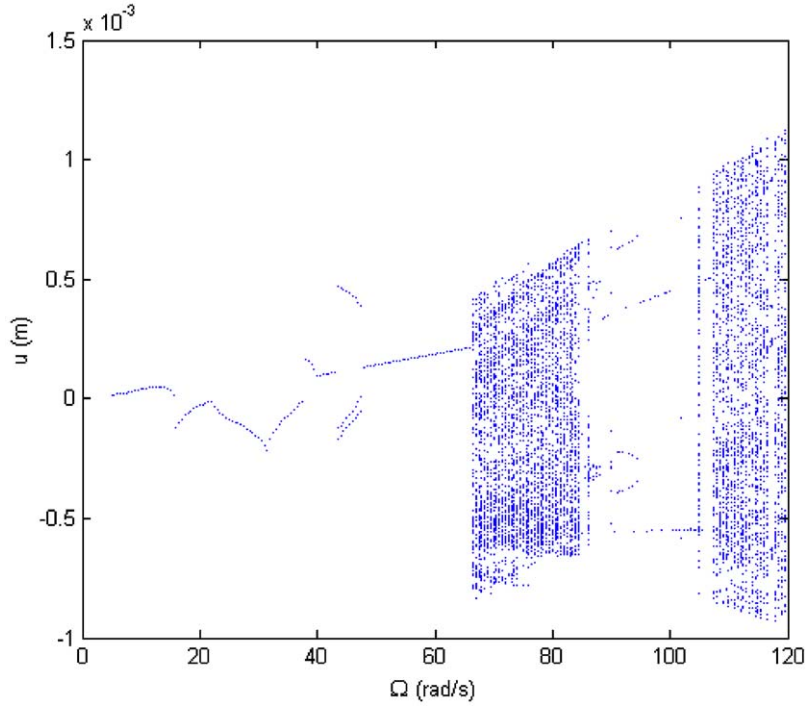

Fig. 20. Bifurcation plot with damping at the lower bound ($K_3 = 5.0e11$ and $C = 30$).

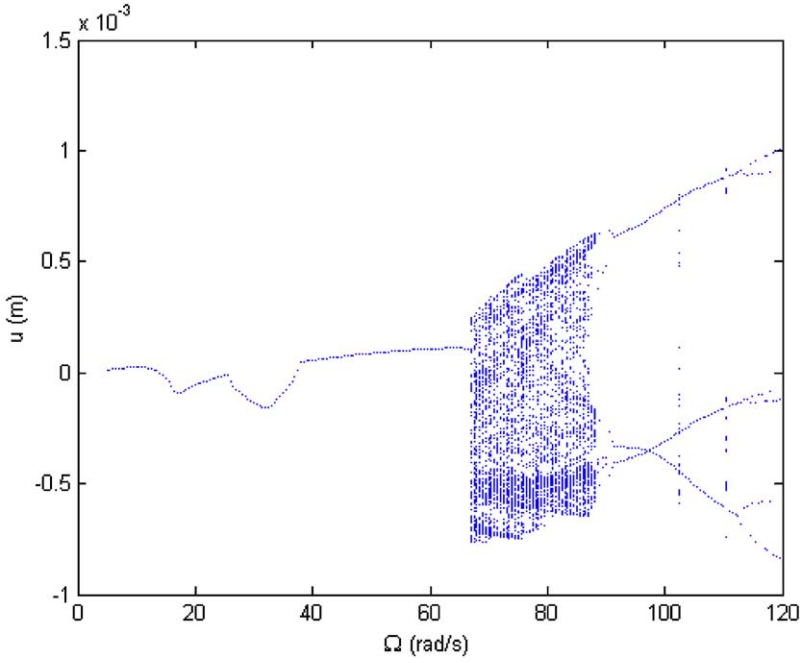

Fig. 21. Bifurcation plot with damping at the upper bound ($K_3 = 5.0e11$ and $C = 90$).

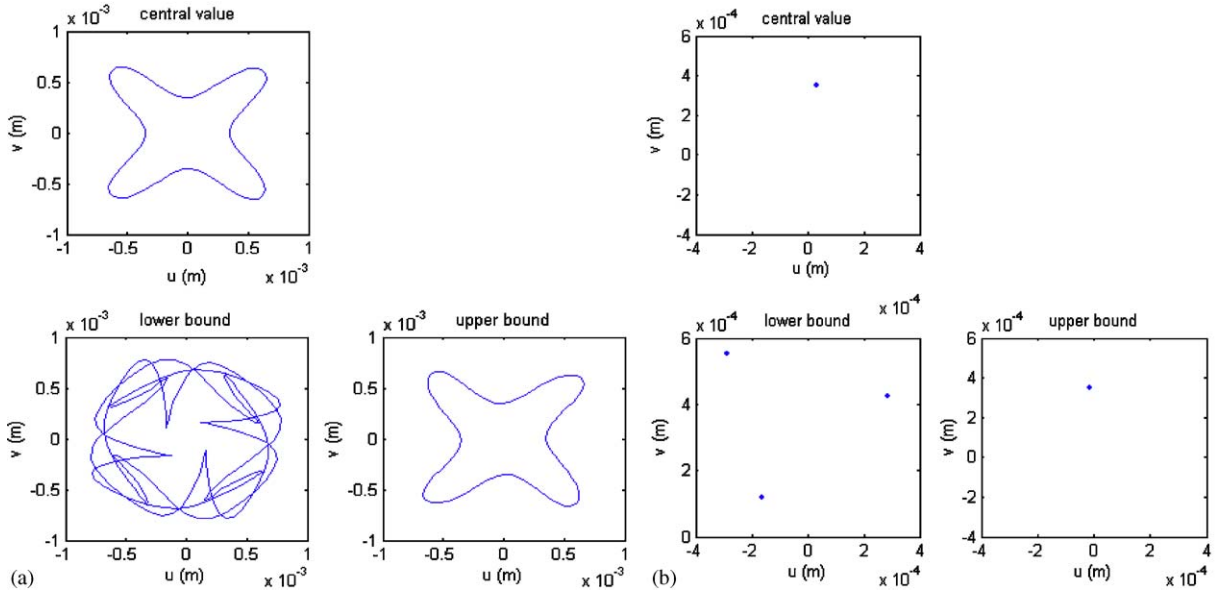

Fig. 22. At rotational speed $\Omega = 45$ rad/s: (a) orbits, and (b) Poincaré map ($K_3 = 5.0e11$ and C is treated as fuzzy).

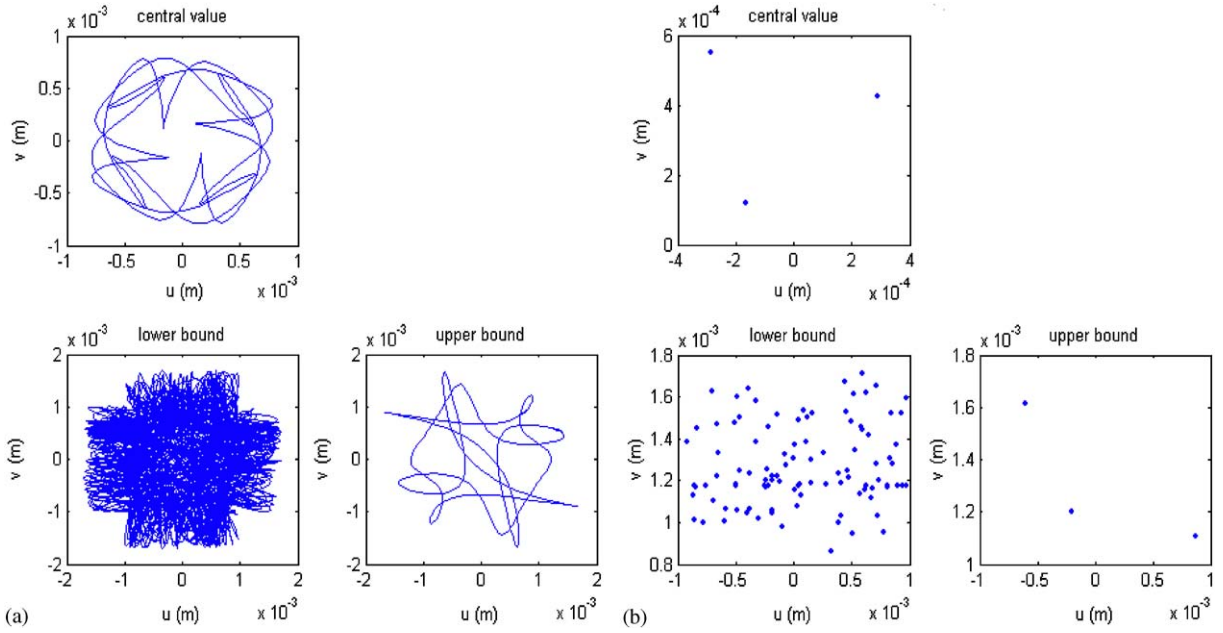

Fig. 23. At rotational speed $\Omega = 111$ rad/s: (a) orbits, and (b) Poincaré map ($K_3 = 5.0e11$ and C is treated as fuzzy).

Table 5
Fuzzy representation of the typical linguistic statement

Set	Linguistic statement	Value of the fuzzy parameter, mass unbalance $me(\times 10^{-5}\,\text{kg m})$					
		1.125	1.250	1.400	1.600	1.800	1.875
		Corresponding membership value					
A	Low	1.0	0.8	0.6	0.4	0.2	0.0
$\bar{A}$	Not low	0.0	0.2	0.4	0.6	0.8	1.0
A^2	Very low	1.0	0.64	0.36	0.16	0.04	0.0
A^4	Very very low	1.0	0.4096	0.1296	0.0256	0.0016	0.0
$\bar{A}^2$	Not very low	0.0	0.36	0.64	0.84	0.96	1.0
B	High	0.0	0.1	0.3	0.6	0.8	1.0
B^2	Very high	0.0	0.01	0.09	0.36	0.64	1.0
$A^2 \cup B^2$	Very low or very high	1.0	0.64	0.36	0.36	0.64	1.0
$A \cap \bar{A}^2$	Low but not very low	0.0	0.36	0.6	0.4	0.2	0.0

linguistic variables. The linguistic variables, including labels such as small, big, low, and high; hedges such as very, quite, and extremely; negation (not); and connections (and, but, or), can be assembled into relatively complex statements such as "very low or not very high", and their fuzzy representations can be compounded with fuzzy arithmetic operations. Fuzzy hedge operations

differ from arithmetic operations because they do not affect the values contained within a fuzzy number; it operates only on the membership function (power of the membership function of fuzzy number A: $\mu_{\text{hedge}}(x) = \left[\mu_A(x)\right]^y$, y is a positive real number) of the fuzzy member A. When y is less than one, it is called concentration; and when y is greater than one, it is called dilation. For example, "low" is a fuzzy set in which all values less than a certain value number are given the membership value of one, and "high" is a fuzzy set in which all values greater than a certain number are given the membership value of one. The fuzzy representation of typical linguistic statements about mass unbalance associated with "low" and "high" are shown in Table 5.

6. Conclusions

A fuzzy approach is presented for the analysis of unbalanced nonlinear rotor systems involving uncertain parameters. The analysis indicates that the uncertainties of a nonlinear rotor-bearing system will not only affect the critical speed, maximum amplitude and jump speed difference, but also the periodic characteristics of the system. The unavoidable uncertainties of the system can lead to unexpected phenomena, which cannot be predicted with a deterministic approach. Since the fuzzy analysis can predict the possible behavior of the system at different confidence levels (corresponding to different values of α cut), the fuzzy approach can be considered to be more versatile and robust in system design and analysis. In the numerical simulations, only one parameter is considered to be fuzzy at a time in order to understand and determine the influence of uncertainties in different parameters. Although triangular membership functions are used for the input fuzzy parameters, the shapes of the membership functions of the response parameters are found to deviate from the triangular form indicating the inherent nonlinearity in the computations. The influence of a combination of several fuzzy parameters can also be studied using the same approach. The Monte Carlo method can be used for computationally intensive cases.

References

[1] Y. Ishida, T. Ikeda, T. Yamamoto, Nonlinear forced oscillations caused by quadratic nonlinearity in a rotating shaft, *Journal of Vibration and Acoustics* 112 (1990) 288–297.
[2] T. Yamamoto, Y. Ishida, *Linear and Nonlinear Rotordynamics. A Modern Treatment with Applications*, Wiley Interscience, New York, 2001.
[3] A. Muszynska, P. Goldman, Chaotic responses of unbalanced rotor/bearing/stator systems with looseness, *Chaos, Solitons and Fractals* 5 (1995) 1683–1704.
[4] A.C. Lee, Y. Kang, S.L. Liu, Steady-state analysis of a rotor mounted on nonlinear bearings by the transfer matrix method, *International Journal of Mechanical Sciences* 35 (1993) 479–490.
[5] E.V. Karpenko, M. Wiercigroch, M.P. Cartmell, Regular and chaotic dynamics of a discontinuously nonlinear rotor system, *Chaos, Solitons and Fractals* 13 (2002) 1231–1242.
[6] Fredic F. Ehrich, *Handbook of Rotordynamics*, McGraw-Hill, New York, 1992.
[7] A.D. Dimarogonas, Interval analysis of vibrating systems, *Journal of Sound and Vibration* 183 (4) (1995) 739–749.
[8] L.A. Zadeh, Fuzzy Set, *Informations and Control* 8 (1965) 338–353.
[9] A. Kaufmann, M.M. Gupta, *Introduction to Fuzzy Arithmetic*, Van Nostrand Reinhold, New York, 1991.

[10] A.-C. Lee, Y. Kang, S.-L. Liu, Steady-state analysis of a rotor mounted on nonlinear bearings by the transfer matrix method, *International Journal of Mechanical Sciences* 35 (6) (1993) 479–490.
[11] Z. Ji, J.W. Zu, Method of multiple scales for vibration analysis of rotor-shaft systems with non-linear bearing pedestal model, *Journal of Sound and Vibration* 218 (2) (1998) 293–305.
[12] S.S. Rao, Description and optimum design of fuzzy mechanical systems, *Journal of Mechanisms, Transmissions and Automation in Design* 109 (1987) 126–132.